High temperature properties of several chromium-containing Co-based alloys reinforced by different types of MC carbides (M=Ta, Nb, Hf and/or Zr)

Patrice Berthod

High temperature properties of several chromium-containing Co-based alloys reinforced by different types of MC carbides (M=Ta, Nb, Hf and/or Zr)

Patrice Berthod

Institut Jean Lamour
Department N°2: Chemistry and Physic of Solids and Surfaces
Team "Surface and interface, chemical reactivity of materials"
Faculty of Sciences and Techniques, Nancy – University,
B.P. 70239, 54506 Vandoeuvre-lès-Nancy – France

Corresponding author's e-mail : patrice.berthod@centraliens-lille.org
Corresponding author's phone: (33)3 8368 4666 and fax number: (33)3 8368 4611

Abstract

Five cast cobalt alloys based on Co-8Ni-30Cr-0.4/0.45C and containing Ta, Nb, Hf and/or Zr were studied by metallography in the as–cast condition and after treatments at 1300°C. The obtained MC carbides were all interdendritic with a eutectic script–like morphology. For similar carbon contents, the HfC carbides are the most developed in the as–cast microstructure and the most stable at 1300°C. As–cast, the TaC carbides are less developed than the former and they tend to become more fractioned and less present in microstructure at 1300°C. The NbC carbides, which have initially the same morphology and the same fraction as TaC, rapidly dissolve at 1300°C. The cobalt alloys containing HfC or TaC are chromia–forming at 1300°C. The NbC–containing alloy catastrophically oxides after only few hours at 1300°C. The average hardness is the highest for the HfC–containing alloy and the lowest for the NbC–containing alloy.

Keywords: High temperature alloys (A); Microstructure (C); Oxidation (C); Thermal analysis (D); Scanning electron microscopy (D)

1. Introduction

The strengthening of some of the alloys or superalloys designed for high temperature applications is due to carbides, and especially to MC carbides which are of the most stable at high temperature (around 1200°C). Among them, the most used in cast alloys is TaC carbide [1], notably in cobalt-based superalloys [2,3]. Tantalum is a carbide–former element which is more efficient than chromium. Therefore TaC carbides can be easily obtained in Cr–rich cobalt alloys instead of chromium carbides [4]. It is also true in chromium–rich ferritic or austenitic alloys based on (Fe,Cr) or (Fe,Ni,Cr) [5,6] but TaC are more difficult to obtain in (Ni,Cr)–based alloys [7].

Among the other MC carbides which can be used for the strengthening of alloys at high temperatures, one can cite firstly NbC. The niobium carbides, which can induce an increase in both hardness and wear resistance of steels [8] or cermets[9], are able to improve the mechanical properties at high temperature of refractory alloys or intermetallics [10]. The HfC carbide is among the most stable ones at very high temperatures. Hafnium carbides are notably used for the mechanical reinforcement of very refractory alloys, based on molybdenum, tungsten and/or rhenium [11–13]. The

zirconium carbide (ZrC) is another MC carbide which is also used in alloys for applications at very high temperatures, for example in Mo-based or Nb-Mo based alloys [14–16].

TaC is the most used MC carbide for strengthening the cast cobalt–based superalloys, while NbC, HfC or ZrC seem being more rarely considered as strengthening particles in such alloys. The purpose of this work is to better know the as–cast microstructures of Co–based alloys containing one or several of these MC–former elements, their refractoriness and their behavior when exposed at very high temperatures.

2. Experimental details of the study

2.1. The studied alloys

Five cobalt–based alloys, all containing about 8 wt.%Ni, 30 wt.%Cr, 0.4 wt.%C and different contents in M elements (M = Ta, Nb, Hf and Zr) were elaborated by high frequency (300kHz) induction melting under an inert atmosphere (0.3 bar of pure argon). The fusion of the charge (total mass ≅ 50g) and solidification of the obtained liquid alloy were realized in the water–cooled copper crucible of the furnace. These alloys are denominated as indicated in Table 1 which also gives the obtained chemical compositions of these alloys, determined by Energy Dispersion Spectrometry for all elements except carbon. The contents in the latter element were assumed being equal to the targeted values, on the one hand since the same elaboration procedure always leads to a very good respect of the carbon content as earlier verified several times by spark spectrometry analysis (technique efficient for this light element even in low contents), and on the other hand since this good respect of the targeted C contents is confirmed by the obtained carbides densities in the alloys studied here.

The obtained ingots were cut in order to obtain compact samples (less than 1 cm^3) for the as–cast microstructures examinations and for the high temperature treatments, as well as smaller parts (about $2 \times 2 \times 8$ mm^3) to measure the intervals of fusion of the alloys.

2.2. Thermal analysis

Differential Thermal Analysis (DTA) experiments were performed on the five alloys, in order to measure their temperatures of fusion's start and of fusion's end. This was done using a Setaram TGA 92-16.18 apparatus, following a thermal cycle composed by a heating rate of 20 K min^{-1} up to 1,200 °C, a slower heating at 5 K min^{-1} up to 1,500 °C for a better accuracy in this zone of temperatures. The cooling was done first at 5 K min^{-1} down to 1,200°C, followed by a second one at 20 K min^{-1} down to room temperature. For the assessment of the solidus and liquidus temperatures of the alloys it was preferred here to consider the temperatures of fusion's start and fusion's end determined on the heating part of the DTA curve. Indeed, taking the values at solidification, or even the average values of start and end of fusion and solidification, may lead to minimized temperatures because of nucleation delay and undercooling during solidification.

2.3. High temperature exposures and metallographic characterization

The samples corresponding to the alloys which presented a melting temperature high enough (higher than 1300°C: "CoTa", "CoNb" and "CoHf"), were polished all around with 1200-grit paper. They were heated in a resistive tubular furnace up to

1,300°C, at approximately 20 K min^{-1}. A first sample was taken out the furnace at the end of heating, a second one after 5 hours spent at 1,300°C and the third one after 20 hours spent at 1,300°C. All of them were then air–cooled down to room temperature. After cutting in two equal parts (using a Buehler Isomet 5000 precision saw), and embedding in a cold resin (Escil CY230 + HY956), the mounted samples were polished, firstly by using SiC paper from 120 to 1,200 grit under water, and secondly with a 1μm–diamond paste.

A Scanning Electron Microscope (SEM, model: XL30 Philips) was used for metallographic observations, essentially in the Back Scattered Electrons mode under an acceleration voltage of 20kV. The region of interest was either the middle of the sample's bulk (characterization of the carbides evolution without influence of oxidation), or the zone affected by oxidation (for characterizing the surface degradation by oxidation). The chemical composition of each alloy was analyzed in the bulk of the as–cast alloy, by using the Energy Dispersion Spectrometry device of the SEM (except for carbon which is a too light element, and which was assumed being equal to the targeted values as already explained above).

The surface fractions of carbides were measured on four BSE micrographs randomly taken in the bulk of each sample (as–cast and for the three durations at 1,300°C). These micrographs were taken with the SEM in BSE mode and a magnification × 250 (areas of almost 0.1mm^2). The BSE detector led to different levels of gray, depending on the average atomic number of the phases. After a careful rating of the brightness/contrast SEM parameters, the matrix (gray) and the MC carbides (whiter than matrix) were then well separated, what allowed the Photoshop CS software of Adobe measuring the surface fractions of carbides, after a rating of gray level avoiding to take into account also carbides close to the sample surface but not really emerging. Each final surface fraction, average of three measures, was supposed to be close to the volume fractions.

2.4. Hardness measurements

In order to know the hardness evolution with the 1300°C–treatment duration, macro-indentation was performed on the three alloys selected for the heat treatments, by using a Testwell Wolpert apparatus. Four Vickers indentations with a load of 30kg were performed in the bulk of each sample, far from the zone affected by oxidation.

2.5. Characterization of surface deterioration by oxidation

The resistance of the alloys against high temperature oxidation was characterized by observing the surface of cross sections of the samples exposed at 1300°C with the SEM in BSE mode, by measuring the depths or thickness of the zone affected by oxidation and by characterizing the oxide scales (thickness, nature and porosity). Electron Probe Micro Analysis (EPMA) was also performed, with a Cameca SX100 apparatus working by Wavelength Dispersion Spectrometry. A short profile was performed per sample through the entire external oxide scale while a longer profile was performed through the entire zone of alloy affected by oxidation. This allowed identifying the natures of the different oxides present.

3. Results

3.1. As–cast microstructures of the studied alloys

The as–cast microstructures of the five alloys are illustrated by SEM micrographs in Fig. 1. The "CoTa" alloy is composed of a dendritic matrix and TaC carbides forming a eutectic with matrix in the interdendritic spaces. The same features are met in the "CoNb" microstructure, with NbC carbides instead of TaC, and in the "CoHf" alloy with HfC carbides. The latter seem to be denser than the interdendritic TaC or NbC carbides of the two former alloys. In addition, one can notice the presence of coarser white particles, especially rich in Hf (and even probably being pure Hf). Indeed their WDS analyses with microprobe showed that they contain more than 95wt.% of Hf, while the other detected elements seemingly belonged to the subjacent matrix which often participates to the interaction with the electrons beam when the analyzed particles are too small. The "CoTH" alloy, which contains both tantalum and hafnium, is also composed of a dendritic matrix and interdendritic carbides, but the latter are less dense and less script–like than in the three previous alloys. The last alloy, "CTHZ" which contains Ta, Hf and Zr together, is especially rich in interdendritic carbides and intermetallic particles which cannot be analyzed because of their too fine structures.

3.2. Results of DTA experiments

Differential Thermal Analysis was carried out for the five alloys. Generally, two endothermic peaks were found in the heating part of the obtained curves while the cooling part of the curves displayed two exothermic peaks, as illustrated in Fig. 2.

The temperatures of fusion's start et fusion's end, which were taken as estimations of the solidus and liquidus temperatures, were measured at the beginning and end of heat absorption. Their values are given in Table 2. Except for the "CTHZ" alloy, all temperatures of fusion's start are equal to 1300°C or higher. In the increasing order, and by considering only the alloys containing one M element, one meets first the TaC–containing alloy, then the NbC–containing alloy and finally the HfC–containing alloy. The alloy containing both Ta and Hf starts melting at almost the same temperature as the "CoTa" alloy. The "CTHZ" alloy, which is obviously too rich in M elements, is the less refractory of the five alloys since it starts melting near 1225°C. Only the alloys displaying both a sufficiently high temperature of fusion's start (equal or higher than 1300°C) and a simple structure of carbides (with only one M element in MC carbides) were considered for the exposures at 1300°C.

3.3. Behaviors of the bulk microstructures during a dwell at 1300°C

Three samples of each considered alloy ("CoTa", "CoNb" and "CoHf") were exposed at 1300°C for three different durations. The less exposed was air-cooled when it reached 1300°C (condition called "0h"), the second one remained at 1300°C during five hours ("5h") and the most exposed one staid at 1300°C during twenty hours ("20h"). The microstructure bulk behaviors of the three alloys were quite different from each other. The TaC network of the "CoTa" alloy, seemed already a little affected when reaching the targeted temperature. The fragmentation and rarefaction of the tantalum carbides were more marked after 5 hours, and, after 20 hours the script–like carbides were totally replaced by aligned blocky TaC carbides (Fig. 3). The same phenomena took place for the "CoNb" alloy, but faster since carbides were already fragmented when reaching 1300°C and they became especially rare after 20 hours (Fig. 4). In contrast the "CoHf" alloy was particularly less affected by time spent at 1300°C (Fig.

5). Indeed, the interdendritic carbide network still existed after 20 hours, even if the fragmentation of the HfC carbides was obvious (but less marked than in the "CoTa" alloy, and of course than in the "CoNb" alloy).

Three pinpoint WDS analysis were performed by EPMA in matrix in the centre of each sample, with calculation of the average value and the standard deviation taken as uncertainty (Table 3). It seems that the chromium content and the nickel content did not change with the exposure duration. In contrast, the Ta content in the "CoTa" matrix and the Hf content in the "CoHf" matrix both tend to decrease (with almost total disappearance of Hf in matrix), while the Nb content seems increasing in the "CoNb" matrix.

3.4. Behaviors of the alloys in oxidation at 1300°C

During the exposures at high temperature the alloys underwent a more or less severe oxidation. The metallographic characterization of the oxidized alloys led to see that the behaviors can be totally different between the three alloys (Fig. 6 and Table 4). The external oxide scale growing on the "CoTa" surface is rather thin at all times and contains an increasing thickness of chromia (Cr_2O_3). Since this stoechiometric oxide is particularly protective, the oxidation of the alloy remains limited, even if a spinel oxide ($CoCr_2O_4$) appeared between 0h and 5h and grew thereafter on the external oxide. Such spinel usually results from the reaction between an inner Cr_2O_3 scale and a (Co,Ni)O outer scale, the latter formed at the first stage of oxidation (but which cannot be seen here probably because it was lost during cooling; in contrast this external divalent oxide is still present in the oxide scales of the two other alloys). Another oxide (internal $CrTaO_4$) grew with time inward the sub-surface: it is the unique penetration of oxidation which can be noted in this "CoTa" alloy. From the extreme surface of the "CoTa" alloy, a depletion in chromium developed inward the centre of the alloy, with a gradient of Cr content which decreases with time. The chromium content on the extreme surface of the alloy decreased from 16 wt.%Cr ("0h") down to 12 wt.%Cr ("20h"). The latter is a very low value which let think that the chromia–forming behavior of the alloy might be lost after only few supplementary hours, and therefore that catastrophic oxidation is imminent. Concerning the microstructure changes induced by oxidation in the alloy sub-surface, it can be noted that a carbide–free zone developed from the external surface, because of diffusion of tantalum toward the oxidation front (where it is oxidized into $CrTaO_4$), leaving carbides which were dissolving over an increasing depth in the alloy. One can notice that the first part of the chromium profile for "20h" (0.039 wt.%Cr $\times$ μm^{-1}) seemingly corresponds to the carbide–free zone depth, while the inner gradient (three times lower than the first gradient) concerns an inner zone where carbides are still present.

The behavior of the "CoNb" alloy is totally different. Chromia existed only when temperature reached 1300°C, and the very low Cr content in extreme surface (7.2 wt.%Cr) explains why the chromia–forming behaviour was thereafter lost and replaced by a general oxidation which penetrated inward the alloy. This catastrophic behavior involved simultaneous oxidation of Cr, Co, Ni and Nb in more or less complex and more or less porous oxide. Chromia did not continue to diffuse and the Cr content remained still close to 30 wt.% at the moving frontier between the growing oxide and the part of alloy which was not yet oxidized.

The "CoHf" alloy displays a behavior which can be intermediate by comparison with the two previous ones. Chromia seems to be almost always present on surface,

covered by the $CoCr_2O_4$ spinel formed by reaction with the outer early (Co,Ni)O oxide (which was sometimes lost during cooling). The Cr gradient exists in the sub–surface of all samples, which proves that Cr continued diffusing toward the oxidation front. The chromium content in the extreme surface decreased down to 8.2 wt.% after 20h at 1300°C, which let think to a loss of the chromia–forming behavior few hours later. There is seemingly never a carbide–free zone in the sub–surface of the three "CoHf" samples, and then no correspondence between Cr gradient and carbide–free zone depth can be done.

3.5. Hardness of the alloys for the different treated states

Vickers indentation was performed four times per sample, with calculations of the average value and of the standard deviation (taken as uncertainty). Results are presented in the graphs displayed in Fig. 8. For an easier interpretation values (average ± standard deviation) of surface fractions measured by image analysis (on three BSE micrographs per sample) are added in these graphs. In the case of the "CoHf" alloy, two curves of surface fraction are plotted: one for the HfC carbides together with the Hf-rich precipitates, and one for only the HfC carbides (nevertheless the two curves are close to one another since the Hf-rich precipitates do not lead to important additional surface fractions). The hardness of the "CoTa" alloy follows the same tendency as TaC surface fractions, i.e. a continuous decrease from 310 down to 295 Hv_{30kg}, for TaC surface fraction decreasing from 7.7 to 4.3 surf.%. The same behavior, but drastically accelerated in time, can be seen for the "CoNb" alloy, with fast decreases in hardness (337 down to 254 Hv_{30kg}) and in NbC surface fraction (4.2 down to 1.1 surf.%). For the "CoHf" alloy, the HfC surface fraction begins increasing from about 8 (as–cast) to about 10 surf.% ("5h") then decreases to about 8 ("20h"). This is the same evolution as the one of hardness that increases from 304 to 331 Hv_{30kg}, then decreases to 301 Hv_{30kg} ("20h").

4. Discussion

Thus, tantalum, niobium and hafnium lead to the same type of as–cast microstructure in a chromium–rich carbon–containing cobalt–based alloy: a dendritic matrix with script–like carbides forming an interdendritic eutectic with matrix. Although the carbon contents of these studied alloys are similar, different densities of interdendritic carbides were obtained. Obviously the carbide network obtained with Hf in the "HfC" alloy is more developed than the TaC network of the "CoTa" alloy, which is itself more developed than the NbC network in the "CoNb" alloy, although the atomic contents of M element (M=Hf, Ta, Nb) were the same. Surprisingly, the combination of Ta and Hf in the "CoTH" alloy, for a same total atomic content of carbide–former elements as the three previous alloys, led to less carbide (in the as–cast condition). The "CTHZ" alloy which contains three times the atomic content of M element in the "CoTa", "CoNb" and "CoHf" alloys, was especially rich in interdendritic carbides, and also in intermetallic compounds (mixed with the carbides) since the carbon content was the same as for all the other alloys. In the latter alloy the interdendritic compounds could be considered as matrix, instead the cobalt solid solution, because of its higher volume fraction.

The alloys with equal atomic contents for carbon and for the M elements present are the most refractory, with temperatures of fusion's start of at least 1300°C. When the atomic content of M elements exceeds too much the carbon atomic content, this

temperature becomes significantly lower, as it is the case for other alloys in which M elements were less present than carbon and in which chromium carbides appeared in microstructures in addition to MC carbides [4].

When exposed at 1300°C, both morphology and surface fraction of carbides are changing. The decrease in surface fraction was fast for the "CoNb" alloy (with consequently an increase in Nb content in matrix), and obviously slower for the "CoTa" alloy (inversely the carbide fraction increased in the "CoHf" alloy). The fragmentation of NbC carbides was also very much faster for NbC than for the two other alloys. The NbC carbides are then not useful for mechanical properties while the other MC carbides seem being potentially able to maintain a significant level of mechanical resistance at high temperature.

The "CoTa" alloy is probably the best one for the resistance against oxidation at high temperature. Indeed oxidation remains essentially on surface, except a growing internal oxidation of both chromium and tantalum into $CrTaO_4$, which is frequent in cobalt alloys reinforced by TaC carbides [17–20]. Even after 20 hours there was no generalized oxidation and the existence of a gradient of chromium content shows that Cr continued to diffuse to maintain the protective chromia scale. The latter unfortunately reacted with the first oxide formed, CoO (more precisely (Co,Ni)O), particularly strongly because of the especially high temperature (1300°C). Thus, the real thickness of protective oxide was lower than what can be expected regarding the chromium quantity which diffused toward the oxidation front. After 20 hours at 1300°C, the chromium content was significantly lowered and catastrophic oxidation appeared to be imminent.

The behavior of the "CoHf" alloy in oxidation is similar to the previous alloy's ones, but it can be thought that the catastrophic oxidation was also imminent, as suggested by the critically low chromium content in extreme surface. The main difference with the "CoTa" alloy is the impossibility of Hf atoms to diffuse toward the oxidation front, i.e. differently to Ta atoms which leaved dissolving TaC carbides and diffused outward to be oxidized into $CrTaO_4$ just under the external surface of the "CoTa" alloy, allowing the development of a carbide–free zone. HfC carbides did not really dissolve, and on the contrary seemed coarsening since the Hf content in matrix, which was already very low in the as–cast microstructure (which also led to Hf-rich precipitates in addition to carbides), continued to decrease during the 1300°C exposures. This suggests that the exposure at 1300°C allowed finishing the formation of the (very stable) HfC carbides from Hf and C atoms initially trapped in matrix by solidification. In addition to its tendency to do not stay in a cobalt–base matrix, even in very small quantity, it seems that Hf atoms cannot diffuse through matrix and also along the interdendritic boundaries, as suggested by the absence of any carbide-free zone. Together with the high stability of the HfC carbides, this can also explain why HfC were much less affected by fragmentation than the other MC carbides. The oxidation of HfC occurred but only in extreme surface, seemingly into a complex oxide involving notably Hf and Cr rather than into HfO_2 to which oxidation of HfC alone can lead [21].

The Vickers hardness at room temperature is clearly related to the surface fraction of carbides, a relationship which can be affected by the degree of fragmentation of the carbides. The latter probably enhances the decrease in hardness when the carbide fraction decreases. The levels of hardness between the three alloys are sensibly different; for all heat treatments together the following order was observed: Hv ("CoNb", except as-cast) < Hv ("CoTa") < Hv ("CoHf"). This can be related to the

carbide volume fractions (Fig. 9), but also to the differences of hardness between the different carbides (TaC: 1800Hv_{50g}, NbC: 2400 Hv_{50g} and HfC: 2900 Hv_{50g} [22]). One might also take into account the differences between the matrixes themselves since their level of strengthening by heavy atoms (atomic weights: Nb < Hf ≈ Ta), which are moreover present in different quantities in solid solution (weight contents in matrix: Ta ≈ Nb >> Hf).

5. Conclusion

Chromium–containing cobalt–based alloys containing MC carbides and elaborated by casting are able to display simultaneously a high refractoriness (if not too rich in M elements) and a network of strengthening carbides which can be sufficiently developed in the interdendritic areas for 0.4-0.5 wt.% of carbon only. The stability of two of the studied carbides at a very high temperature (1300°C), and then the efficiency of strengthening they may bring, can be good (TaC) or very good (HfC), although the fragmentation phenomenon, faster for TaC than for HfC, probably reduces high temperature strength as it lowers hardness at room temperature. In addition, the resistance of the corresponding alloys against high temperature oxidation can be maintained at a high level for several tens hours (chromia–forming behavior). In contrast, NbC in a cobalt alloy cannot be exposed at high temperature without quick dissolution and early catastrophic oxidation (after only few hours at 1300°C). Among the three MC carbides tested here in a cast cobalt–based alloy, the one containing HfC seems the most able for applications at very high temperatures (even around 1300°C).

Acknowledgements

The author thanks the Common Service of Microanalysis of the Faculty of Science and Techniques of the University Henri Poincaré Nancy 1 for the EPMA measurements.

References

[1] C. T. Sims, W. C. Hagel, The Superalloys, John Wiley & Sons, 1972.
[2] A.M. Beltran; in C.T. Sims, N.S. Stoloff, W.C. Hagel, Superalloy II – High temperature materials for aerospace and industrial power, John Wiley, New York, 1987, pp. 135-163.
[3] S. Michon, P. Berthod, L. Aranda, C. Rapin, R. Podor, P. Steinmetz, Calphad 27 (2003) 289-294.
[4] P. Berthod, S. Michon, L. Aranda, S. Mathieu, J.C. Gachon, Calphad 27 (2003) 353-359.
[5] P. Berthod, Y. Hamini, L. Aranda, L. Héricher, Calphad 31 (2007) 351-360.
[6] P. Berthod, Y. Hamini, L. Héricher, L. Aranda, Calphad 31 (2007) 361-369.
[7] P. Berthod, L. Aranda, C. Vébert, S. Michon, Calphad 28 (2004) 159-166.
[8] W. Theisen, S. Siebert, S. Huth; Steel Research International 78 (2007) , 921-928.
[9] S.G. Huang, L. Li, O. Van der Biest, J. Vleugels, Journal of Alloys and Compounds 430 (2007) 158-164.
[10] W.Y. Kim, H. Tanaka, S. Hanada, Materials Transactions, 43 (2002) 1415-1418.
[11] A. Luo, J.J. Park, D.L. Jacobson, B.H. Tsao, M.L. Ramalingam, Scripta Metallurgica et Materialia, 29 (1993) 729-732.
[12] Y. Ozaki, R.H. Zee; Scripta Metallurgica et Materialia, 30 (1994) 1263-1267.
[13] J.J.Park; International Journal of Refractory Metals & Hard Materials, 17 (1999) 331-337.
[14] T. Takida, M. Mabuchi, M. Nakamura, T. Igarashi, Y. Doi, T. Nagae, Metallurgical and Materials Transactions A, 31 (2000) 715-721.
[15] Y. Tan, C.L. Ma, A. Kasama, R. Tanaka, J.M. Yang, Materials Science and Engineering A, 355 (2003) 260-266.
[16] Y. Tan, C.L. Ma, R. Tanaka, J.M. Yang, Materials Transactions, 47 (2006) 1527-1531.
[17] J. Di Martino, S. Michon, L. Aranda, P. Berthod, R. Podor, C. Rapin, Ann. Chim. Sci. Mat. 28 (Suppl. 1) (2003) S231-S238.
[18] P. Berthod, S. Michon, S. Mathieu, R. Podor, C. Rapin, P. Steinmetz, Materials Science Forum, 461-464 (2004) 1117-1124.
[19] P. Berthod, S. Raude, A. Chiaravalle, A.S. Renck, C. Rapin, R. Podor, Rev. Met. CIT/Sci. Mater. 12 (2004) 1031-1042.
[20] P. Berthod, S. Raude, A. Chiaravalle, Ann. Chim. Sci. Mat. 31 (2) (2006) 237-258.
[21] S. Shimida, Solid State Ionics, 141-142 (2001) 99-104.
[22] Handbook of High-Temperature Materials – Materials Index, Plenum Press, 1964.

TABLES

Table 1
Chemical compositions of the studied alloys
(SEM/EDS, ± 1wt.% for all elements except C*)

Alloys	Co	Ni	Cr	C*	Ta	Nb	Hf	Zr
CoTa	Bal.	8.1	29.4	0.39*	6.5	/	/	/
CoNb	Bal.	8.1	29.7	0.46*	/	3.3	/	/
CoHf	Bal.	7.7	30.0	0.43*	/	/	6.6	/
CoTH	Bal.	8.3	31.0	0.41*	3.2	/	3.0	/
CTHZ	Bal.	8.3	29.8	0.40*	6.4	/	6.0	3.1

*: targeted contents, supposed well respected (as usually verified for such alloys and this elaboration procedure)

Table 2
Values of the solidus temperatures and liquidus temperatures determined on the heating part of the DTA curves

Alloys Temperatures	"CoTa"	"CoNb"	"CoHf"	"CoTH"	"CTHZ"
Tliq (°C)	1450	1402	1421	1429	1311
Tsol (°C)	1300	1310	1322	1300	1226

Table 3
Chemical composition of the matrix in the centre of all samples exposed at 1300°C

Alloy	wt.%Cr		wt.%Ni		wt.%Ta	
"CoTa"	average	± std dev.	average	± std dev.	average	± std dev.
"0h"	30.48	± 0.21	8.43	± 0.07	2.10	± 0.11
"5h"	30.85	± 0.22	8.48	± 0.31	1.90	± 0.03
"20h"	29.87	± 0.39	8.54	± 0.38	1.87	± 0.26

Alloy	wt.%Cr		wt.%Ni		wt.%Nb	
"CoNb"	average	± std dev.	average	± std dev.	average	± std dev.
"0h"	31.21	± 0.14	8.61	± 0.07	1.26	± 0.19
"5h"	30.60	± 0.12	8.66	± 0.12	2.11	± 0.17
"20h"	30.94	± 0.02	8.55	± 0.16	2.29	± 0.24

Alloy	wt.%Cr		wt.%Ni		wt.%Hf	
"CoHf"	average	± std dev.	average	± std dev.	average	± std dev.
"0h"	31.82	± 0.25	8.33	± 0.01	0.29	± 0.20
"5h"	31.52	± 0.59	8.12	± 0.35	0.08	± 0.07
"20h"	28.85	± 0.76	8.18	± 0.24	0.02	± 0.02

Table 4
Natures and thicknesses of oxides scales, chromium contents in the most external zone of alloy and chromium gradients in sub-surface, after oxidation at 1300°C

zone	**oxide**			**substrate / bulk**		
sample	3rd scale	2nd scale	1st scale or internal oxidation	Cr mini d_{cfz}	wt.% Cr × µm^{-1}	
					1st zone	2nd zone
CoTa 0h	/	Cr_2O_3 6µm	$CrTaO_4$ (int. ox.)	16.0wt.% 25 µm	0.130 over 48 µm	/
CoTa 5h	$CoCr_2O_4$ 4µm	Cr_2O_3 15µm	$CrTaO_4$ (int. ox.)	15.6wt.% 72µm	0.146 over 130 µm	/
CoTa 20h	$CoCr_2O_4$ 18µm	Cr_2O_3 40µm	$CrTaO_4$ (int. ox.)	12.0 wt.% 338µm	0.039 over 320 µm	0.013 over 460 µm
CoNb 0h	/	Ox. of Cr-Co-Ni-Nb 15µm	Cr_2O_3 7µm	7.2 wt.% no c.f.z.	0.855 over 20µm	0.298 over 20µm
CoNb 5h	(Co,Ni)O 50µm	Oxide of Cr-Co-Ni-Nb compact 50µm	porous 240µm	29.4 wt.% no c.f.z.	0.024 over 40µm	/
CoNb20h	(Co,Ni)O 120µm	Oxide of Cr-Co-Ni-Nb compact 180µm	porous 760µm	23.3 wt.% no c.f.z.	0.175 over 40µm	/
CoHf 0h	(Co,Ni)O 19µm	Ox. of Cr-Co-Ni-Hf 9µm	Cr_2O_3 8µm	13.4 wt.% no c.f.z.	0.498 over 20µm	0.241 over 30µm
CoHf 5h		(Co,Ni)O 16µm	$CoCr_2O_4$ 15µm	16.9 wt.% no c.f.z.	0.127 over 120µm	/
CoHf 20h		$CoCr_2O_4$ 8µm	Cr_2O_3 6µm	8.2 wt.% no c.f.z.	0.171 over 100µm	0.050 over 100µm

FIGURES

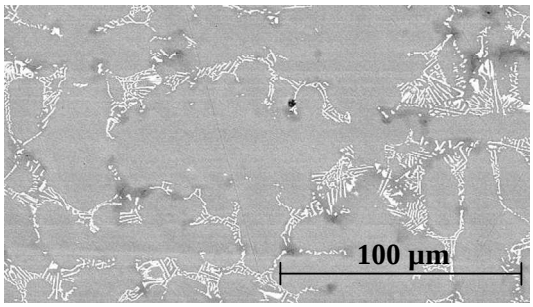

CoTa

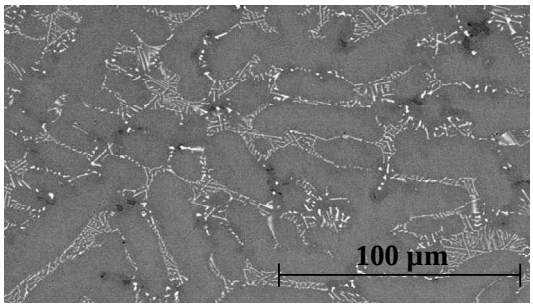

CoNb

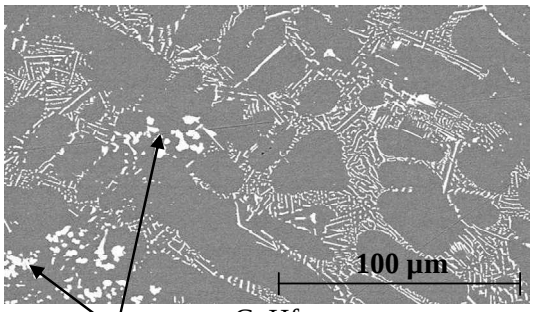

CoHf

Hf-rich precipitates

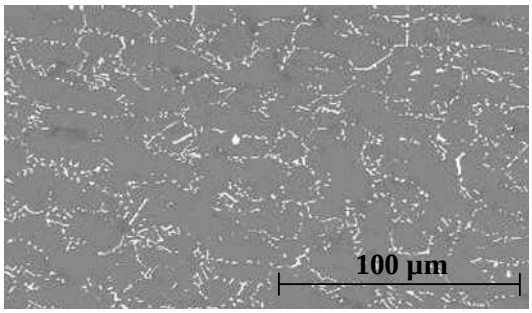

CoTH

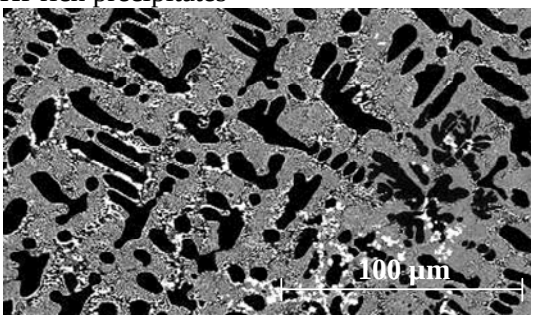

CTHZ

Fig. 1.
Microstructures of the five studied alloys in the as–cast condition
(SEM/BSE micrographs)

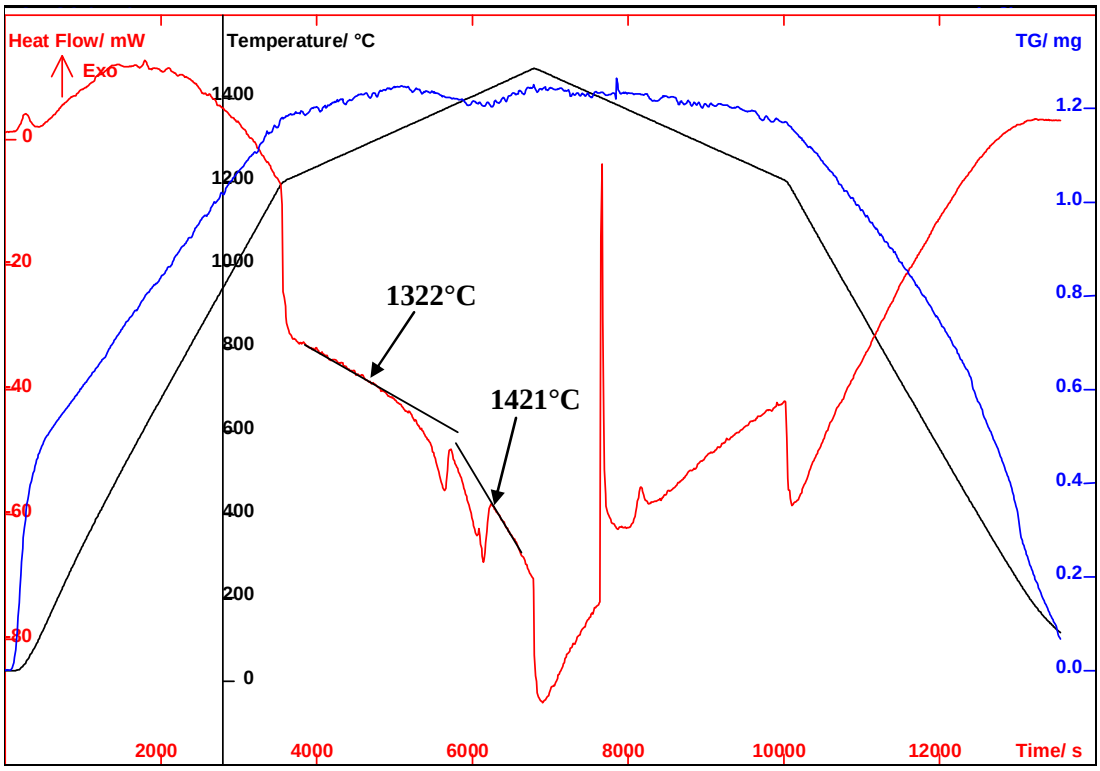

Fig. 2. Example of DTA curve (here: "CoHf" alloy), with determination of the temperatures of fusion's start and fusion's end
(supposed close to the solidus and liquidus temperatures)

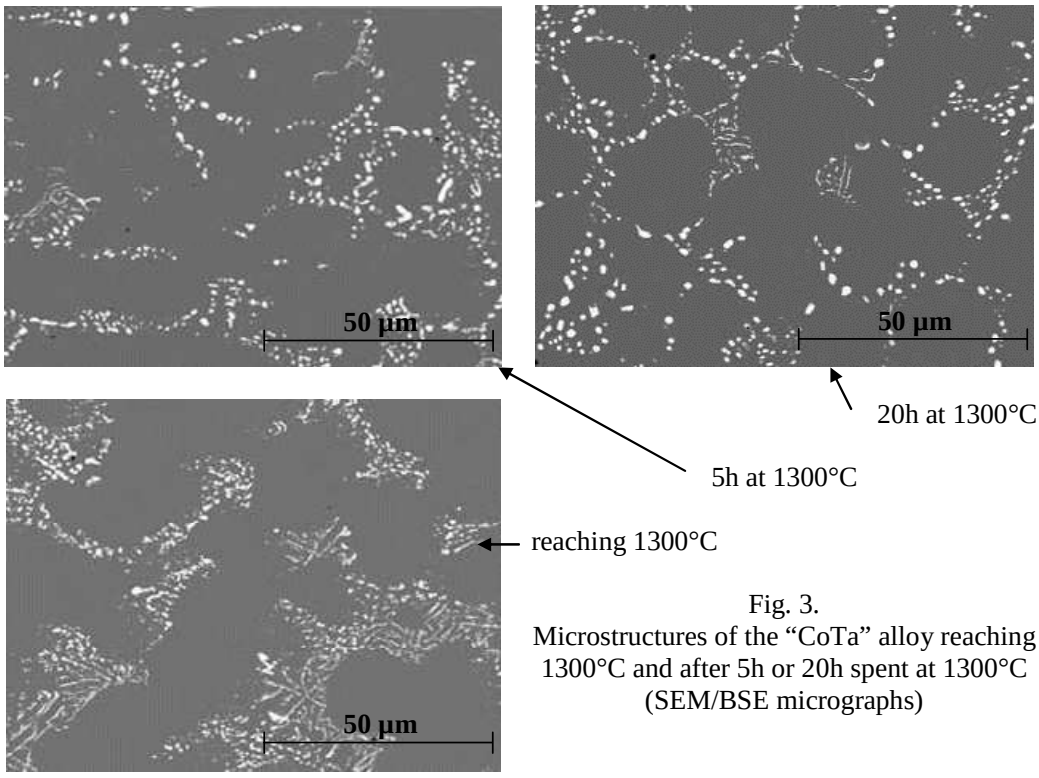

Fig. 3.
Microstructures of the "CoTa" alloy reaching 1300°C and after 5h or 20h spent at 1300°C
(SEM/BSE micrographs)

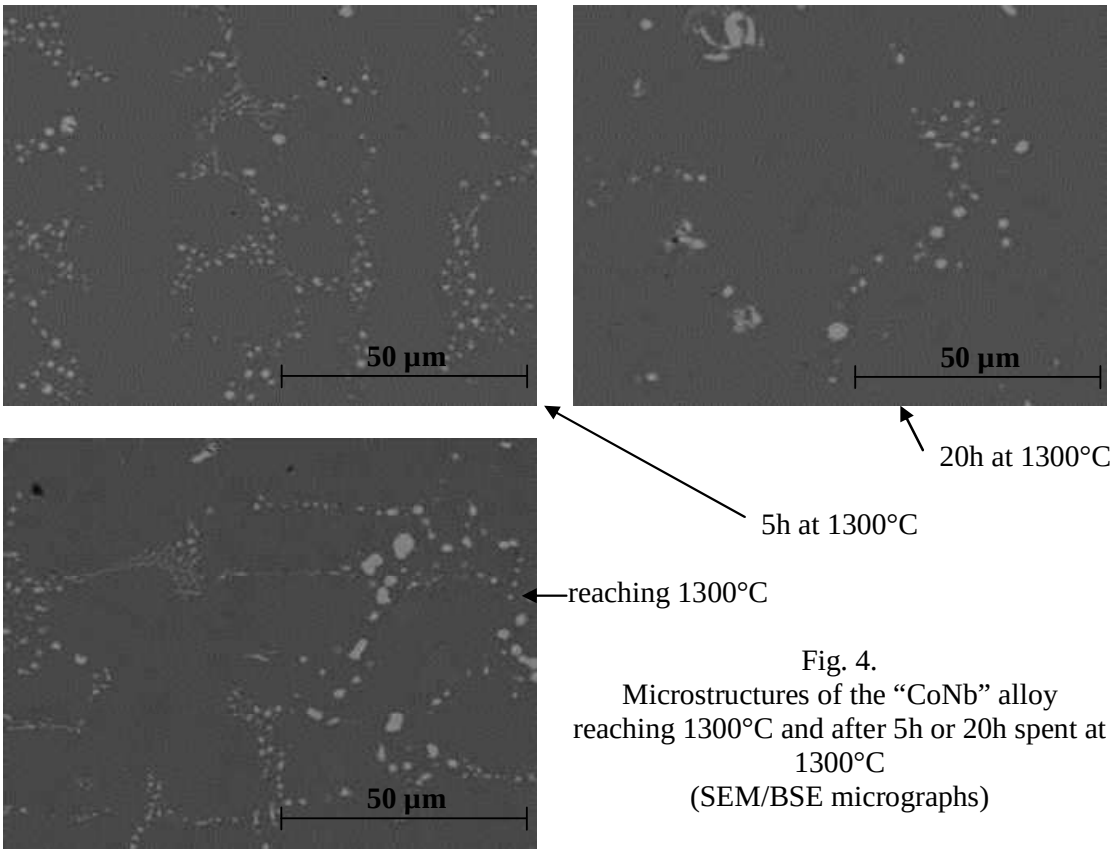

Fig. 4.
Microstructures of the “CoNb” alloy reaching 1300°C and after 5h or 20h spent at 1300°C
(SEM/BSE micrographs)

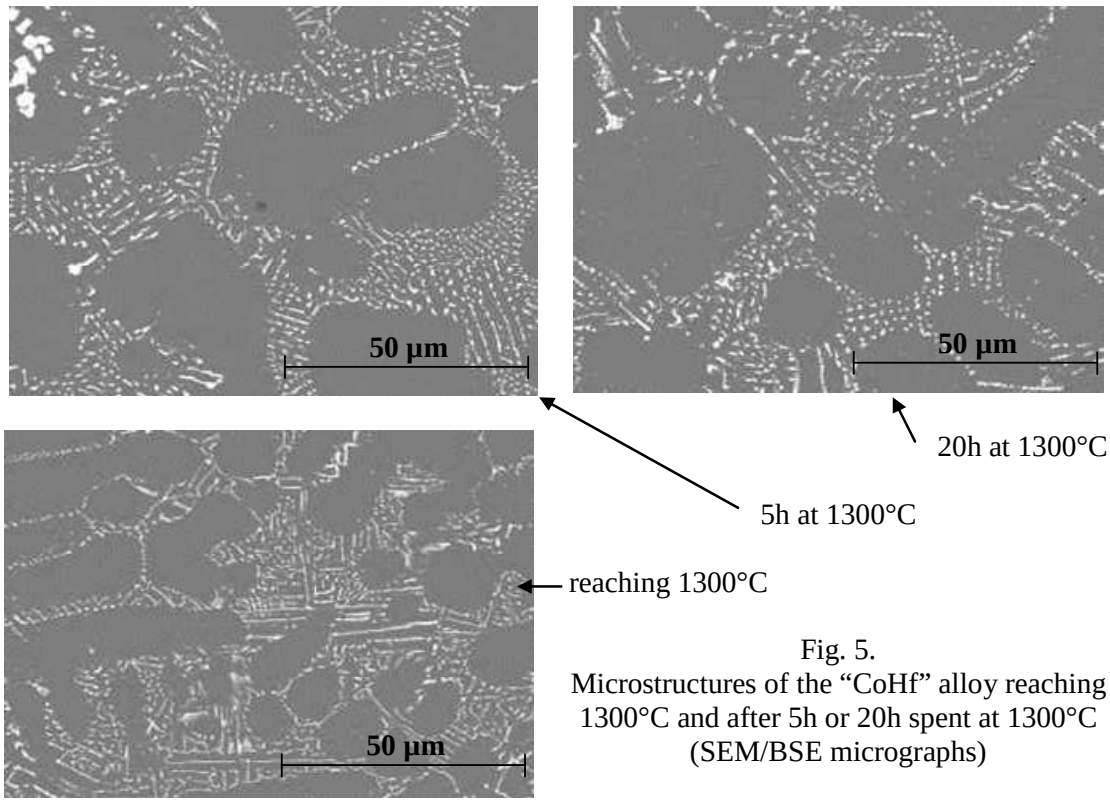

Fig. 5.
Microstructures of the “CoHf” alloy reaching 1300°C and after 5h or 20h spent at 1300°C
(SEM/BSE micrographs)

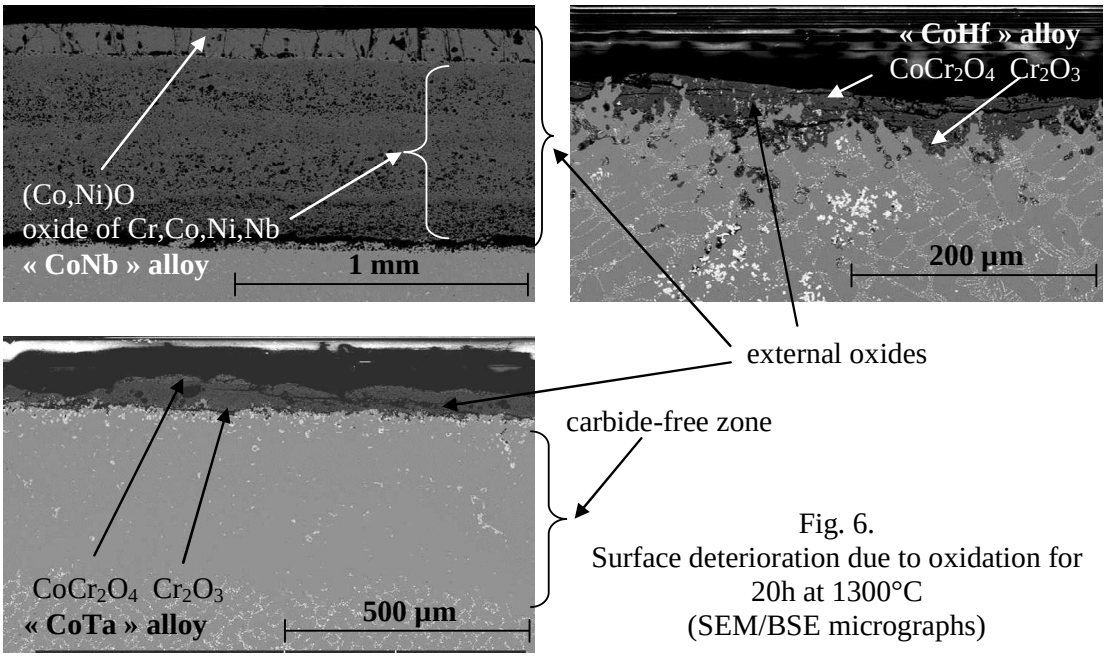

Fig. 6.
Surface deterioration due to oxidation for 20h at 1300°C
(SEM/BSE micrographs)

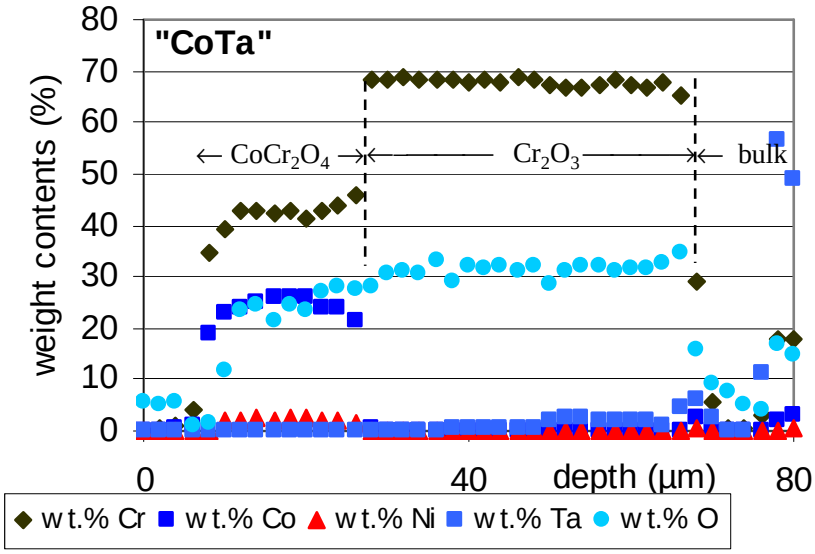

Fig. 7a. Contents profiles through the oxides scales of “CoTa” oxidized during 20 hours at 1300°C (EPMA WDS profiles)

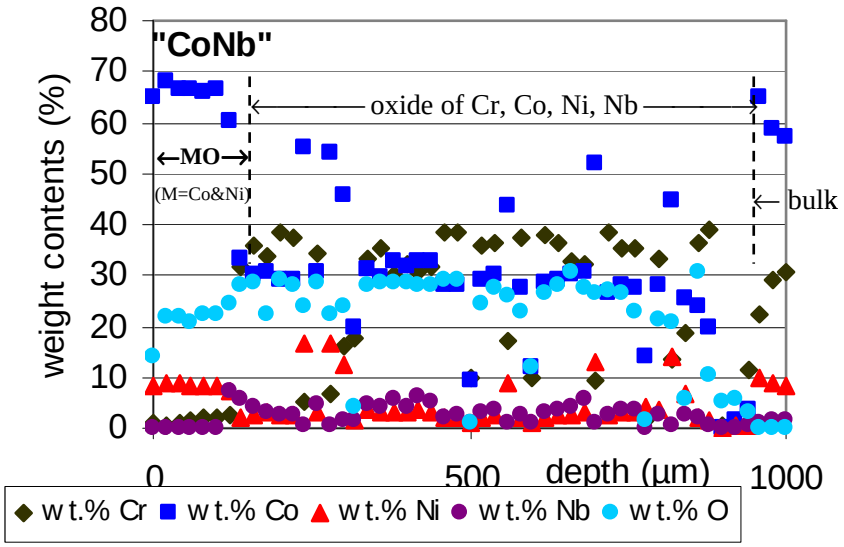

Fig. 7b. Contents profiles through the oxides scales of “CoNb” oxidized during 20 hours at 1300°C (EPMA WDS profiles)

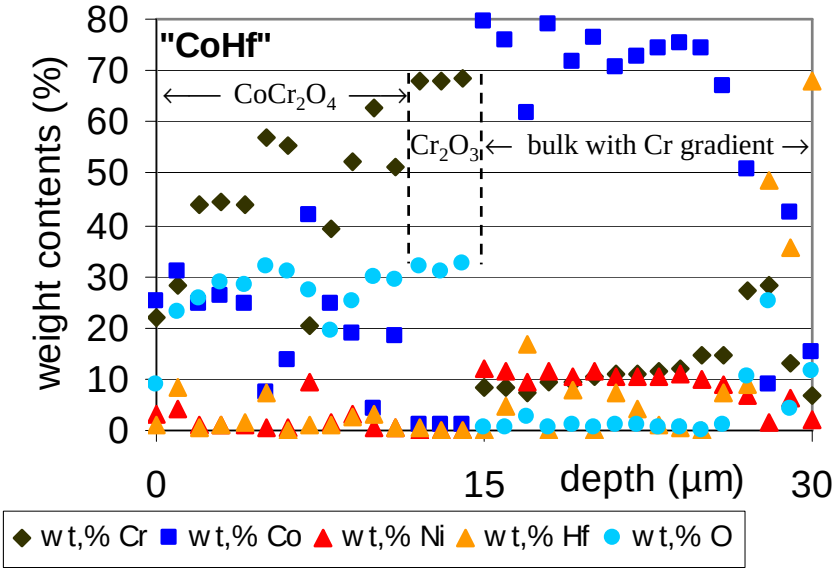

Fig. 7c. Contents profiles through the oxides scales of “CoHf” oxidized during 20 hours at 1300°C (EPMA WDS profiles)

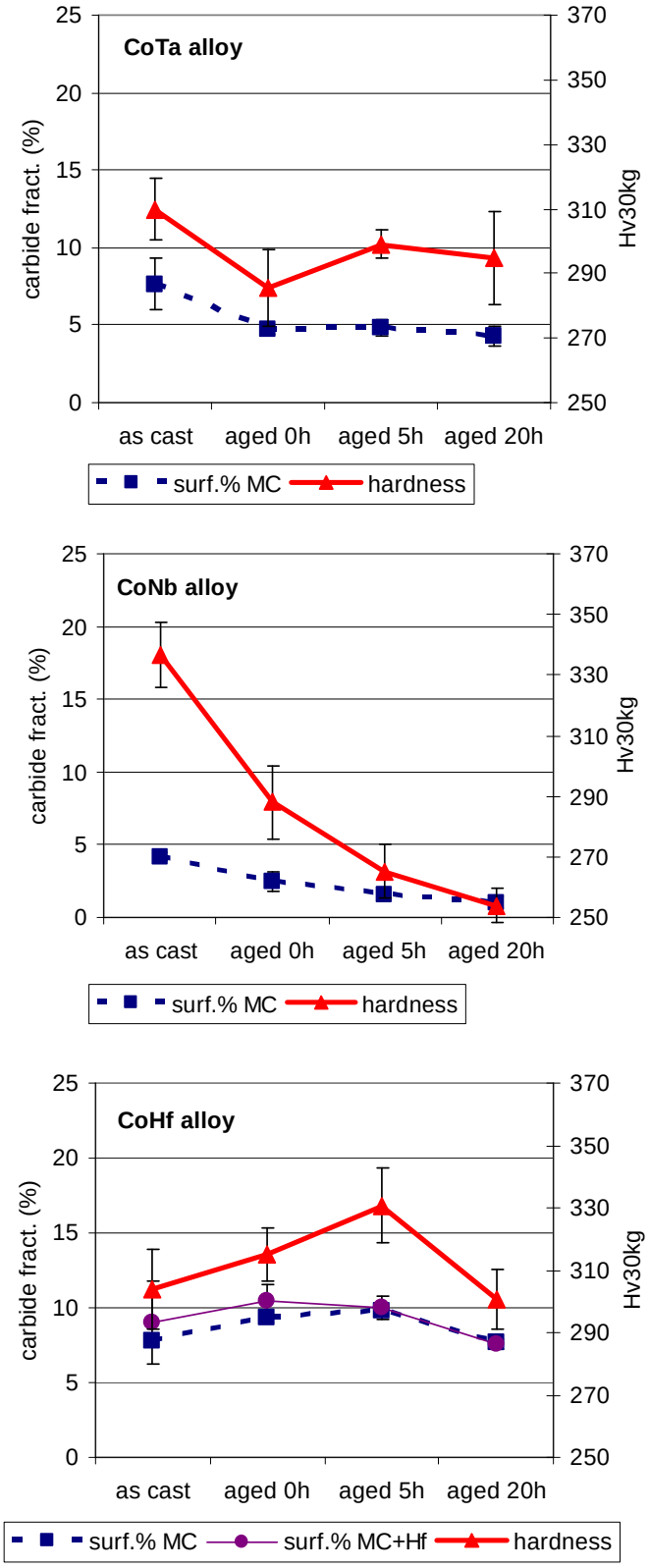

Fig. 8. Surface fractions of MC-carbides and Vickers hardness (30kg) in the alloys for the four states (as cast and aged for “0h”, 5h and 20h at 1300°C

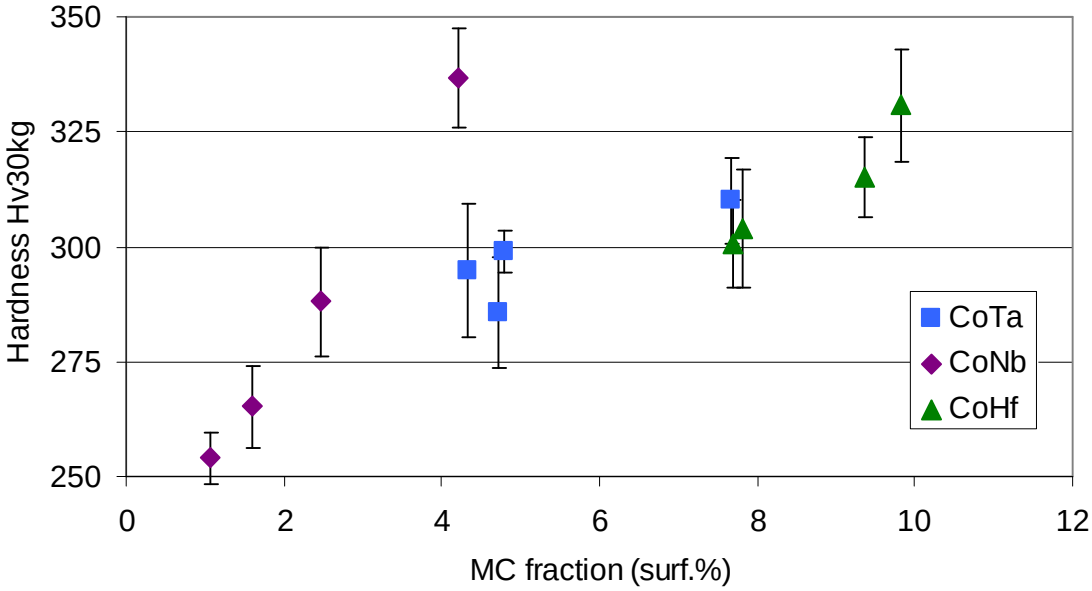

Fig. 9. Vickers Hardness versus MC surface fraction for all alloys and all treated states